ADVANCED FUNCTIONAL MATERIALS
www.afm-journal.de

Materials Views
www.MaterialsViews.com

High-Performance All-Solid-State Cells Fabricated With Silicon Electrodes

Viet Phong Phan, Brigitte Pecquenard, and Frédéric Le Cras**

All solid-state thin-film lithium microbatteries are a promising component able to fulfill most of the specific requirements to power autonomous microsystems. Nevertheless, metallic lithium, which is commonly used as the negative electrode in microbatteries, has a very low melting temperature (T_m = 181 °C) that appears to be incompatible with the solder-reflow operation (maximum temperature $T_{max} \approx$ 260 °C) usually used to connect electronic components. Silicon is a promising candidate to replace lithium in solder-reflowable lithium-ion cells due to its high volumetric capacity (834 μAh cm^{-2} μm^{-1} for $Li_{15}Si_4$) and its ability to reversibly insert lithium at a low potential. Nevertheless, it suffers from a large volumetric expansion during lithium insertion (280%), which is partly responsible for a rapid capacity fading when cycled in liquid electrolyte. In this study, all-solid-state Li/LiPONB/Si cells are prepared using physical vapor deposition (PVD) techniques. The cycle life and the coulombic efficiency are found to be excellent in these solid-state cells with almost no loss during 1500 cycles. Despite the large volume expansion due to lithium insertion confirmed by scanning electron microscopy, no evidence of cracks is found in the film or at the electrode/electrolyte interface, even after 1500 cycles.

1. Introduction

The recent development of numerous miniaturized electronic systems has induced a strong demand for specific energy storage devices. All-solid-state thin-film lithium microbatteries are currently a promising component able to fulfill most of the specific requirements and to power several microdevices including real-time clock controllers, radio-frequency identification tags, stand-alone microelectromechanical systems, medical implants, etc.

Metallic lithium is currently the most used material as the negative electrode in microbatteries, the presence of a dense inorganic glassy electrolyte preventing any dendrites formation.[1–3] Nevertheless, some constraints inherent to the integration process disqualify metallic lithium. In particular, the solder-reflow operation used to weld components needs a thermal treatment at 260 °C, whereas the melting temperature of lithium is only 181 °C.

Consequently, elements able to form alloys with lithium and with melting temperatures above 300 °C constitutes substitutes to lithium in such systems. Among them, silicon which is extensively studied as negative electrode for Li-ion conventional cells is a promising candidate due to its high volumetric specific capacity (834 μAh cm^{-2} μm^{-1} for $Li_{15}Si_4$), its ability to insert/deinsert lithium at a low average voltage (around 0.4 V) and its ability to be prepared by sputtering, a technique widely spread in microelectronics industry.[4,5] Nevertheless, this high volumetric capacity in the non-lithiated state is correlated with a tremendous volume change during lithium insertion (increase of ≈280%).[6] This behavior is generally at the origin of a severe capacity fading, due to the formation of cracks and disintegration of both the active material and the electrode as well as a resulting loss of electrical contacts, with these phenomena being amplified by the reactivity with liquid electrolytes.

To limit the consequences of the volume expansion and thus obtain improved capacity retention, several approaches were followed. In powder-based silicon anodes, the reduction of silicon particle size to nanometers is somewhat helpful.[7] A significant improvement in capacity retention is noticed for composite electrodes prepared with various conductive materials such as carbon.[8] Carbon generates an adherent conductive network, which results in a better electronic connection between the active particles inside the negative electrode. The influence of the binder on the cycle life was also evaluated, with a beneficial replacement of PVDF (polyvinylidene fluoride) by CMC (carboxymethyl cellulose), PAA (polyacrylic acid), or PVA (polyvinyl alcohol).[9–12]

Compared to powder-based silicon negative electrodes, thin film electrodes always show better cycling stability.[5] Among the numerous thin films that were studied, 50 nm amorphous n-type silicon deposited by vacuum deposition on nickel foil showed a stable reversible capacity close to 3500 mAh g^{-1} maintained during 200 cycles under 2C current rate due to their microstructural stability, a greater adhesion to the current

Dr. V. P. Phan
ST Microelectronics SAS
16 rue Pierre et Marie Curie, 37000 Tours, France
Dr. V. P. Phan, Dr. B. Pecquenard
CNRS, Université de Bordeaux
ICMCB (site de l'ENSCPB), 87 avenue du Dr. Schweitzer
33608 Pessac cedex, France
E-mail: pecquen@icmcb-bordeaux.cnrs.fr
Dr. F.Le Cras
CEA LITEN,
17 rue des martyrs, 38054 Grenoble cedex, France
E-mail: frederic.lecras@cea.fr

DOI: 10.1002/adfm.201200104

© 2012 WILEY-VCH Verlag GmbH & Co. KGaA, Weinheim

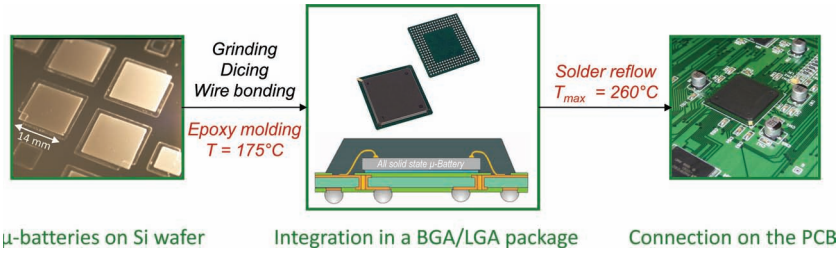

Figure 1. All-solid-state microbatteries and their main processing steps for on-board applications.

collector, and a shorter lithium diffusion pathways in these films.[13] The benefit use of roughened substrate as well as the vinylene carbonate (VC) additive in the electrolyte was demonstrated for thin films.[14,15] This latter point confirms that, similarly to graphite, the nature (composition and morphology) of the solid electrolyte interface (SEI) formed on silicon electrodes has also a great influence on their cycle life.[16,17] Nevertheless the mechanism of degradation is quite different. In the case of silicon, it is mainly connected to liquid electrolyte penetration and deposition of solid reaction products inside fresh cracks generated in the electrode, contributing to its mechanical destruction. Moreover, to take advantage of the better capacity retention of silicon thin films in liquid electrolyte and to achieve higher capacities per current collector area unit, new specific substrates with developed surface areas such as carbon nanowire carpets or metal nanoflakes are used.[18,19]

In the present work, the strategy to improve electrochemical performances consists to avoid the use of a liquid electrolyte which contributes to electrode degradation, by preparing for the first time, all-solid-state cells including a vitreous inorganic electrolyte thin film. Accordingly, this study reports on the development of Li/lithium phosphorus oxynitride doped with boron (LiPONB)/Si stacks by sputtering and evaporation, on thorough electrochemical performances investigation of amorphous Si thin films when integrated in lithium microbatteries.

2. Results and Discussion

A photograph of some Li/LiPONB/Si all-solid-state cells is presented on **Figure 1** and the process generally used to integrate a microbattery on a microelectronic circuit is also shown. The structural properties of silicon and LiPONB thin films were studied by X-ray diffraction in grazing incidence and by transmission electron microscopy, which evidences an amorphous character (data not shown here). The electrochemical behavior of the sputtered Si thin films was studied using cyclic voltammetry at 10 mV h^{-1} in a liquid electrolyte and with the LiPONB solid electrolyte between 50 mV and 1 V vs Li/Li^+ to avoid the crystallization of the $Li_{15}Si_4$ phase evidenced by Obrovac.[20] Similar lithium alloying/dealloying steps were evidenced for both types of electrolyte (**Figure 2**). The associated current peaks are respectively located around 290, 240, and 80 mV. For the first insertion in the all-solid-state cell, a very sharp peak is observed at 290 mV leading to a low irreversible capacity (less than 5% i.e., ≈1 µAh cm^{-2}). As this intense peak is not observed in liquid electrolyte, we can attribute it to the reduction of a reaction product (containing oxidized Si) formed during the solid electrolyte deposition at the interface between silicon and LiPONB thin films. Besides, it was previously shown that the reduction of SiO occurs around 250 mV/Li^+/Li.[21,22] For subsequent cycles, a peak is still observed at the same voltage but with a much reduced intensity. In addition, a very weak reduction peak is observed for both types of electrolyte around 500 mV. It corresponds to a small irreversible reaction independent on the substrate and electrolyte nature and needs to be attributed.

The cycling performances obtained between 50 mV and 1 V are shown on **Figure 3** for an all-solid-state cell having an area equal to 0.94 cm^2. In this potential range, avoiding the formation of crystallized $Li_{15}Si_4$, we do evidence an excellent cycling stability over 1500 cycles at around 100% depth of discharge (DOD) leading to a surface capacity close to 40 µAh cm^{-2},which

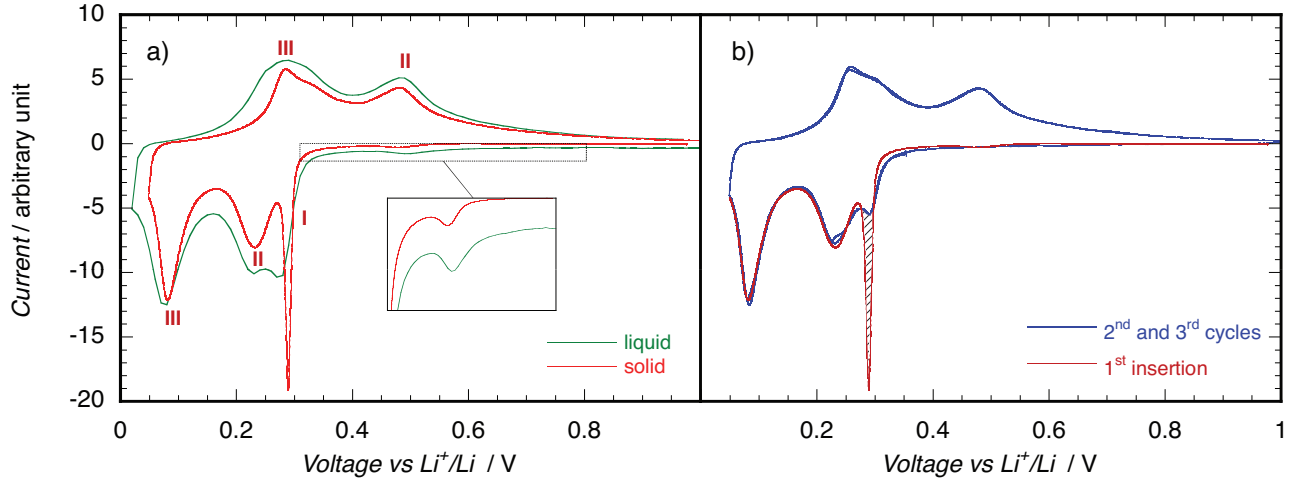

Figure 2. a) Comparison of voltammograms of silicon thin film electrodes in liquid or solid electrolyte during the first insertion/deinsertion cycle. b) Evolution of the voltammogram of a Li/LiPONB/Si cell showing the presence of an irreversible process during the first lithium insertion step.

© 2012 WILEY-VCH Verlag GmbH & Co. KGaA, Weinheim

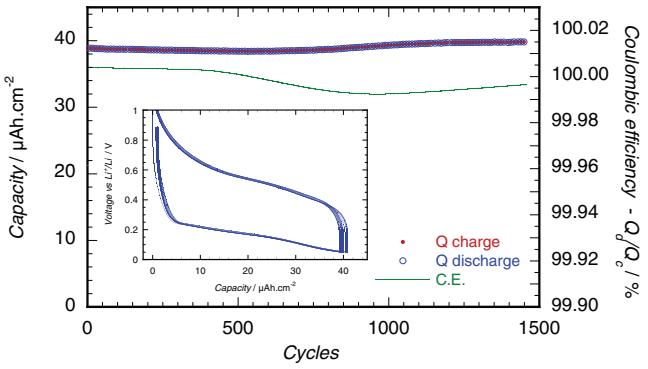

Figure 3. Cycling performance at room temperature of a silicon thin film electrode embedded in an all-solid-state stack. The applied current density is 100 µAh cm^{-2} corresponding to a 2C rate. Inset: the corresponding voltage curves.

corresponds to a volumetric capacity of 571 µAh cm^{-2} µm^{-1} with almost no decrease of the capacity. We can even notice a slight increase of the capacity after 800 cycles. In the insert of the Figure 3, the corresponding charge–discharge curves are almost superimposed for all the 1500 cycles. In addition, the coulombic efficiency is very close to 100% all over the 1500 cycles. Due to lower ionic conductivity of LiPONB solid electrolyte compared to a liquid one, a higher polarization is observed for the all-solid-state system inducing a slightly reduced capacity for given voltage window and current density.

A scanning electron microscopy (SEM) image of the cross-section of the solid cell after 1500 cycles shows no evidence of any mechanical damage (**Figure 4**a). This means that even if a large volume expansion occurs during lithium insertion as confirmed by SEM pictures done on cross-sections of as-prepared and after the first lithium insertion down to 0.05 V (vs Li$^+$/Li) of a Li/LiPONB/Si(400 nm) cell (Figure 4b), no drastic evolution of the electrolyte film nor the electrode/electrolyte interface is observed. This is probably not so surprising if we consider that in lithium microbattery, a similar behavior occurs for metallic lithium thin film except that the initial step consists of contracting the volume of the latter and further expanding it during the charge. Indeed, if we schematically compare the volumetric variation occurring in a Li thin film electrode and a Si electrode between its lithiated and delithiated state for an equivalent surface capacity arbitrary chosen equal to 206 µAh cm^{-2} (**Figure 5**), it clearly appears that the absolute volumetric variation is 30% lower for the silicon, the corresponding thickness variation (Δe) being equal to 693 nm, instead of 1000 nm for the lithium electrode.

Then during the discharge of the cell, lithium is transferred from the negative electrode to the positive one, which respectively shrinks or swells and vice versa during the charge. The overall volume of the stack almost does not vary, and the Li_xSi/LiPONB and Li/LiPONB interfaces move freely and perpendicularly to the substrate. Consequently, a possible damage that could occur would be located on the edges of the stack, where the lithium film goes down onto the wafer surface and is connected to the current collector: the swelling of the stack could eventually break the electrical contact with the negative electrode. This was not observed in these experiments. The high reversibility of the lithium insertion/deinsertion in the silicon thin film appears to be a consequence of a combination of beneficial effects and optimized conditions. The silicon obtained by sputtering is amorphous, which favors isotropic volume changes, the planar geometry of the cell induces the uniaxial swelling and a simple displacement of the interfaces film perpendicularly to the substrate. Finally the use of a true solid electrolyte is the key point. Contrary to what happens in liquid electrolyte, the electrolyte/electrode reactivity does not lead to additional products formed at the surface of the electrode during the electrochemical cycles. Moreover the mechanical properties of the LiPONB film and its strong adhesion to the Si film prevent the initiation of cracks, especially during the delithiation step. Apart from these

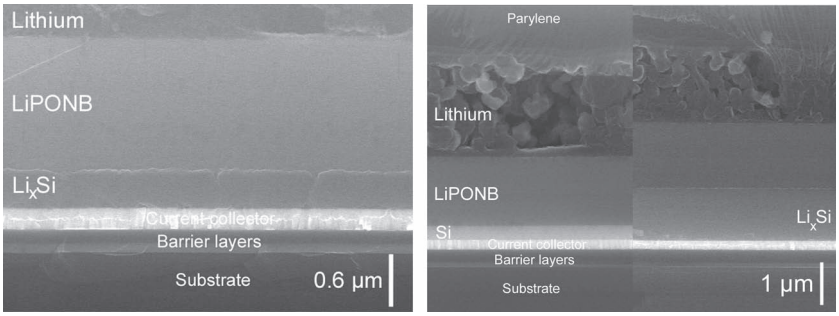

Figure 4. SEM cross-sections images of all-solid-state cells a) after 1500 galvanostatic cycles between 0.05 and 1 V. The initial thickness of the silicon film was 100 nm. b) Comparison between the initial state (left) and after one full discharge down to 0 V/Li$^+$/Li (right).

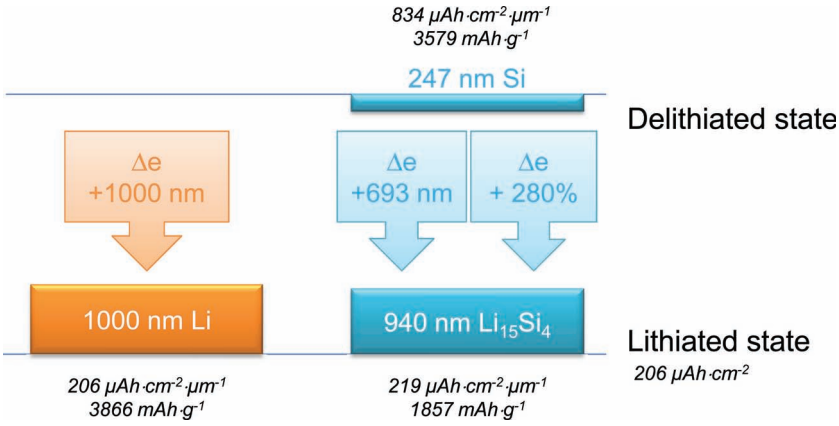

Figure 5. Comparison of the theoretical thickness (or volume) variations of lithium and silicon negative electrodes between the fully delithiated and fully lithiated states for a given available capacity per area unit.

© 2012 WILEY-VCH Verlag GmbH & Co. KGaA, Weinheim

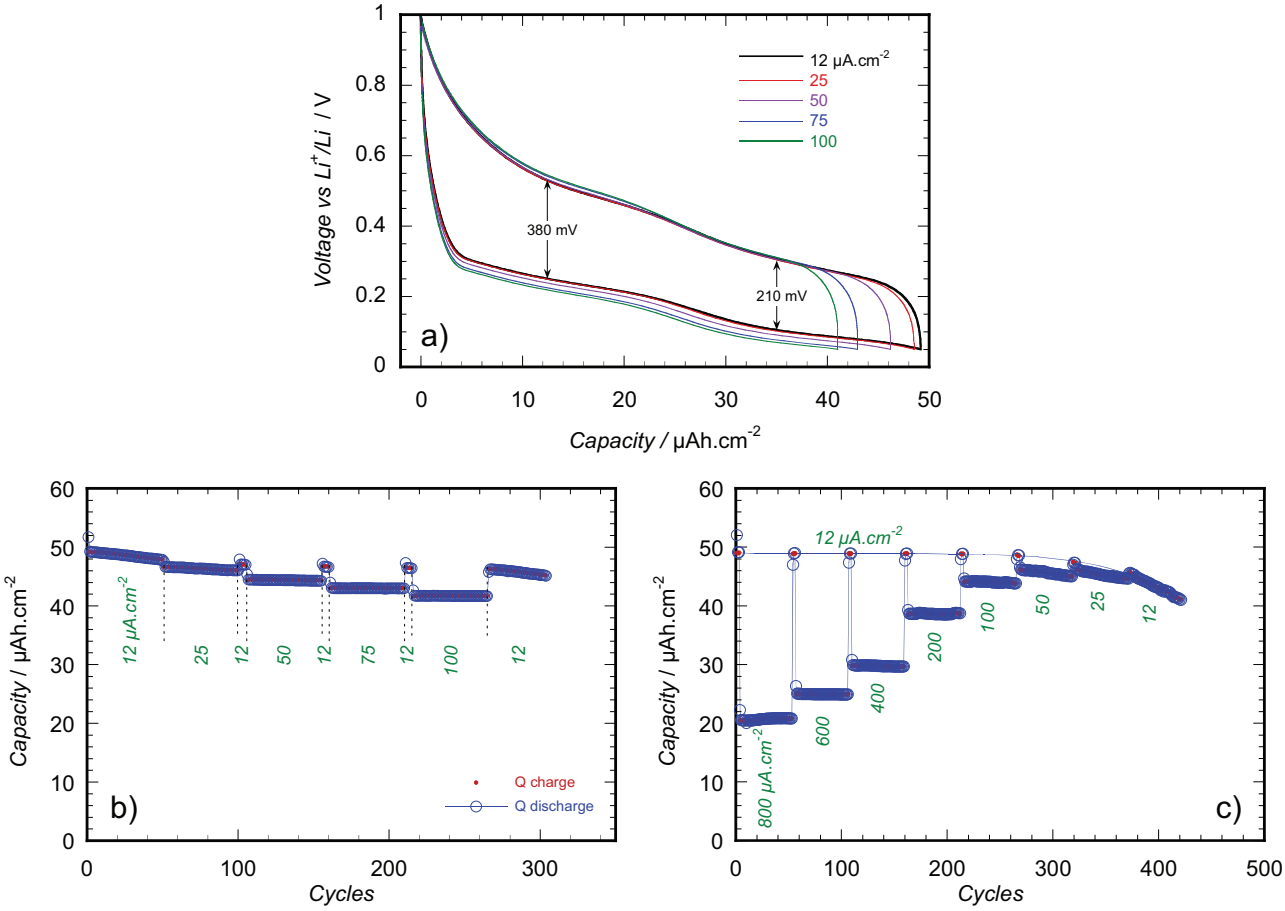

Figure 6. a) Voltage curves of a Si/LiPONB/Li cell cycled at different current densities. Capacity retention obtained between 0.05 to 1.0 V/Li^+/Li b) during a progressive increase of the current density or c) during a top-down sequence. A regular control of the capacity is performed at low current density (12 µA cm^{-2}).

generic features, some parameters were optimized in order to strengthen the cell during operation: the LiPONB thickness (1.4 µm) was high enough to get a good mechanical strength, the choice of the lower cut-off voltage (0.05 V/Li^+/Li) prevented the crystallization of the $Li_{15}Si_4$ phase and the occurrence of additional stress, and the thickness of the Si thin film remained limited to around 100 nm but compatible with the capacity of microbattery applications.

Charge–discharge cycles were carried out on Li/LiPONB/Si cells in the potential range (50 mV to 1 V) by increasing the current densities from 12 µA cm^{-2} to 100 µA cm^{-2}, with 10 intermediate cycles at 12 µA cm^{-2} before each current increase (**Figure 6**). On Figure 6a, we only observe a limited increase of the polarization between insertion and deinsertion process. The main part of this polarization (≈210 mV observed even at low current) is intrinsically due to the lithium insertion in silicon, the extra amount linearly varying with the applied current, being due to ohmic drop (the slope is consistent with the ionic resistivity of LiPONB). Figure 6b shows a highly stable capacity versus cycles at higher rates (above 50 µA cm^{-2}) whereas a quite high capacity fading is observed for lower rates. To better extend the electrochemical characterization, galvanostatic cycling was performed at various rates in the reverse way starting from high current density and then progressively decreasing the latter (Figure 6c). The all-solid state cell was able to be charged and discharged even at a very high current density equal 800 µA cm^{-2} corresponding to a 17C rate. We also obtained the same trend for higher capacity fading at lower rates (typically <100 µA cm^{-2}).

3. Conclusion

All-solid-state cells were fabricated with silicon negative electrode by sputtering and evaporation on 4 inch silicon wafers covered beforehand with barrier layers and current collectors. Excellent performances in terms of cycle life and coulombic efficiency were obtained with almost no loss of capacity and a coulombic efficiency remaining higher than 99.99% over 1500 cycles when cycled between 50 mV and 1 V vs Li^+/Li. Despite the large volume expansion of the silicon thin film electrode no evidence of cracks or damage was observed in the SEM iamges, even after 1500 cycles. Moreover, despite a well-known low lithium diffusion coefficient, the cells was successfully charged and discharged at a very high current density (17C rate). Even if similar lithium alloying/dealloying mechanisms are observed when the

© 2012 WILEY-VCH Verlag GmbH & Co. KGaA, Weinheim

Table 1. Description of the microbattery stack and of its synthesis conditions.

Material	Thickness [µm]	Film manufacturing process
Silicon wafer	500	NA
Barrier layers	0.240	Low-pressure chemical vapor deposition (CVD)
W	0.250	Sputtering
		DC mode – Power density $P = 2.8$ W cm^{-2}, Total pressure $P_{tot} = 0.9$ Pa, Ar 100% Deposition rate = 25 nm min^{-1}
Si	0.100–0.400	Sputtering
		DC mode – $P = 0.34$ W cm^{-2}, $P_{tot} = 0.5$ Pa, Ar 100%
		Deposition rate = 13 nm min^{-1}
LiPONB	1.400	Sputtering
		RF mode – $P = 2.0$ W cm^{-2}, P_{tot}= 2 Pa, N_2 100%
		Deposition rate = 5 nm min^{-1}
Li	3.000	Thermal evaporation
		Deposition rate = 60 nm min^{-1}
Parylene C	5.000	CVD
		$P_{tot} = 3–4 \times 10^3$ Pa, T = room temperature
		Deposition rate = 33 nm min^{-1}

silicon electrode is cycled in liquid and solid electrolyte, this study clearly evidences the beneficial effect of the solid electrolyte and the promising use of silicon in all-solid-state cells.

4. Experimental Section

The all-solid-state half-cells were fabricated by sputtering and evaporation on a 4 in. silicon wafer substrate covered by barrier layers. Each thin film of the half-cell was sequentially deposited, a tungsten current collector, an amorphous silicon electrode, a LiPONB electrolyte, and an evaporated lithium thin film. The deposition parameters are summarized in **Table 1**. The 0.95 Li_3PO_4-0.05 $LiBO_2$ sputtering target was prepared by cold pressing and sintering. The addition of a few percent of boron into the well-known LiPON electrolyte helps to enhance its chemical and thermal stability while maintaining good electrical performance.[23] The substrate was water-cooled during all the deposition process. Cells having various areas respectively equal to 0.21, 0.94, and 1.87 cm^2 were prepared by patterning each film level either by photolithography or shadow masking. The encapsulation of the cells was carried out by polymer/metal thin films multilayer, reinforced by a glass slide for long duration cycling.

Si thin film was also deposited on a roughened copper disk substrate for the electrochemical characterization achieved with a liquid electrolyte and Li negative electrode in order to compare the behavior of the film in a liquid and a solid electrolyte. The coin cells in 316L stainless steel were assembled in a glove box with a Li foil (Chemetall Foote Corp., battery grade 99.9%) as the negative electrode, a liquid electrolyte (1 M $LiPF_6$ in a mixture of ethylene carbonate (EC):propylene carbonate (PC):dimethyl carbonate (DMC) 1:1:3 containing 2% of vinylene carbonate (VC) additive), and a microporous polypropylene separator (Celgard 2400). The electrochemical characterizations were carried out by cyclic voltammetry at a low sweep rate (10 mV h^{-1}), and galvanostatic cycling at 100 µAh cm^{-2} in the potential window (0.05 V to 1 V vs Li^+/Li) for the standard conditions. Some additional galvanostatic measurements were achieved at various current densities from 10 to 800 µA cm^{-2}.

The thin film surface and cross-section were investigated by SEM using a Carl Zeiss Leo 1530 Field Emission Scanning Electron Microscope.

Acknowledgements

The authors thank Nicolas Dunoyer for technical assistance and STMicroelectronics for financial support.

Received: January 12, 2012
Revised: February 21, 2012
Published online: March 29, 2012

[1] S.-W. Song, H. Choi, H. Y. Park, G. B. Park, K. C. Lee, H.-J. Lee, *J. Power Sources* **2010**, *195*, 8275.
[2] B. Fleutot, B. Pecquenard, F. Le Cras, B. Delis, H. Martinez, L. Dupont, D. Guy-Bouyssou, *J. Power Sources* **2011**, *196*, 10289.
[3] C. Navone, R. Baddou-Hadjean, J. P. Pereira-Ramos, R. Salot, *J. Electrochem. Soc.* **2009**, *156*, A763.
[4] J. P. Maranchi, A. F. Hepp, P. M. Kumta, *Electrochem. Solid-State Lett.* **2003**, *6*, A198.
[5] U. Kasavajjula, C. Wang, A. J. Appleby, *J. Power Sources* **2007**, *163*, 1003.
[6] L. Y. Beaulieu, T. D. Hatchard, A. Bonakdarpour, M. D. Fleischauer, J. R. Dahn, *J. Electrochem. Soc.* **2003**, *150*, A1457.
[7] H. Guo, H. Zhao, C. Yin, W. Qiu, *Mater. Sci. Eng. B* **2006**, *131*, 173.
[8] M. Yoshio, T. Tsumura, N. Dimov, *J. Power Sources* **2006**, *163*, 215.
[9] J. Li, R. B. Lewis, J. R. Dahn, *Electrochem. Solid-State Lett.* **2007**, *10*, A17.
[10] B. Lestriez, S. Bahri, I. Sandu, L. Roué, D. Guyomard, *Electrochem. Commun.* **2007**, *9*, 2801.
[11] N. Ding, J. Xu, Y. X. Yao, G. Wegner, I. Lieberwirth, C. H. Chen, *J. Power Sources* **2009**, *192*, 644.
[12] H.-K. Park, B.-S. Kong, E.-S. Oh, *Electrochem. Commun.* **2011**, *13*, 1051.
[13] S. Ohara, J. Suzuki, K. Sekine, T. Takamura, *J. Power Sources* **2004**, *136*, 303.
[14] T. Takamura, M. Uehara, J. Suzuki, K. Sekine, K. Tamura, *J. Power Sources* **2006**, *158*, 1401.
[15] L. Chen, K. Wang, X. Xie, J. Xie, *J. Power Sources* **2007**, *174*, 538.
[16] Y.-C. Yen, S.-C. Chao, H.-C. Wu, N.-L. Wu, *J. Electrochem. Soc.* **2009**, *156*, A95.
[17] M. Ulldemolins, F. Le Cras, B. Pecquenard, V. P. Phan, L. Martin, H. Martinez, *J. Power Sources* **2012**, *206*, 245.
[18] J.J. Nguyen, K. Evanoff, W. J. Ready, *Thin Solid Films* **2011**, *519*, 4144.
[19] M. Saito, K. Nakai, T. Yamada, T. Takenaka, M. Hirota, A. Kamei, A. Tasaka, M. Inaba, *J. Power Sources* **2011**, *196*, 6637.
[20] M. N. Obrovac, L. Christensen, *Electrochem. Solid-State Lett.* **2004**, *7*, A93.
[21] J.-H. Kim, C.-M. Park, H. Kim, Y.-J. Kim, H.-J. Sohn, *J. Electroanal. Chem.* **2011**, *661*, 245.
[22] T. Kim, S. Park, S. M. Oh, *J. Electrochem. Soc.* **2007**, *154*, A1112.
[23] M. Martin, O. Blandenet (HEF), *Patent WO 2005/050764*, **2005.**

© 2012 WILEY-VCH Verlag GmbH & Co. KGaA, Weinheim